HHS Public Access

Author manuscript

Micron. Author manuscript; available in PMC 2021 March 01.

Published in final edited form as:

Micron. 2020 March ; 130: 102822. doi:10.1016/j.micron.2019.102822.

Biophysical Changes Caused by Altered MUC13 Expression in Pancreatic Cancer Cells

Andrew E. Massey[a,b], **Kyle A. Doxtater**[a,b], **Murali M. Yallapu**[a,b,c], **Subhash C. Chauhan**[a,b,c,*]

[a]Department of Pharmaceutical Sciences, College of Pharmacy, University of Tennessee Health Science Center, Memphis, TN, 38163

[b]Department of Immunology and Microbiology, School of Medicine, University of Texas Rio Grande Valley, McAllen, TX, 78504

[c]South Texas Center of Excellence in Cancer Research, School of Medicine, University of Texas Rio Grande Valley, McAllen, TX, 78504

Abstract

Background—Pancreatic cancer is one of the most lethal cancers in the United States. This is partly due to the difficulty in early detection of this disease as well as poor therapeutic responses to currently available regimens. Our previous reports suggest that mucin 13 (MUC13, a transmembrane mucin common to gastrointestinal cells) is aberrantly expressed in this disease state, and has been implicated with a worsened prognosis and an enhanced metastatic potential in PanCa. However, there is virtually no information currently to describe the biophysical ramifications of this protein.

Methods—To demonstrate the biophysical effect of MUC13 in PanCa, we generated overexpressing and knockdown model cell lines for PanCa and subsequently subjected them to various biophysical experiments using atomic force microscopy (AFM) and cellular aggregation studies.

Results—AFM-based nanoindentation data showed significant biophysical effects with MUC13 modulation in on PanCa cells. The overexpression of MUC13 in Panc-1 cells led to an expected decrease in modulus, and a corresponding decrease in adhesion. With MUC13 knockdown, HPAF-II cells exhibited an increased modulus and adhesion. These results were confirmed with altered cell-cell adhesion as seen with aggregation assays.

[*]Correspondence and requests for materials should be addressed to: **Subhash C. Chauhan, PhD**, Professor and Chair, Department of Immunology and Microbiology, Founding Director, Institute for Cancer Immunology, University of Texas Rio Grande Valley School of Medicine, 5300 North L Street, Room 1.202, McAllen, TX 78504, Phone: (956)-296-5000, subhash.chauhan@utrgv.edu.

Author contributions

Conception and design: S.C. Chauhan, A.E. Massey
Development of methodology: A.E. Massey, K. A. Doxtater, S.C. Chauhan
Acquisition of Data: A.E. Massey, K.A. Doxtater
Interpretation of Data: A.E. Massey, K.A. Doxtater, M.M. Yallapu, S.C. Chauhan,
Writing of manuscript: A.E. Massey, S.C. Chauhan, M.M. Yallapu
Study Supervision: S.C. Chauhan

Conclusions—MUC13 led to significant biophysical changes in PanCa cells and which exhibited characteristic phenotypic changes in cells demonstrated in previous work from our lab. This work gives insight into the use of biophysical measurements that could be used to help diagnose or monitor cancers as well as determine the effects of genetic alterations at a mechanical level.

Graphical Abstract

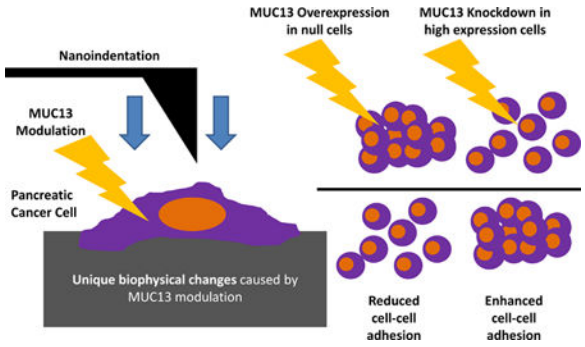

Keywords

MUC13; pancreatic cancer; nanoindentation

1. Introduction

Pancreatic cancer (PanCa) remains one of the deadliest cancers and leading causes of cancer-related death in the United States, requiring additional research to improve quality of life and survival rates. As of 2018, over 44,000 deaths were estimated out of around 55,000 new cases representing a nearly 80% mortality rate.[1] Even with recent advances in surgical techniques, chemotherapeutic regimens and radiation therapies, there is a poor 5-year survival rate of less than 10%.[2] One critical factor in this disease is the aberrant expression of various mucins.[3] These high molecular weight glycoproteins are normally expressed on the exterior of mucosal surfaces to act as a protective barrier with the surroundings.[4]

One mucin of note is MUC13, a transmembrane mucin which is normally expressed at low levels in the large intestine, trachea, kidney, small intestine, and gastric epithelium. Current evidence in the literature suggests an aberrant expression of MUC13 has been associated with ovarian and gastrointestinal cancers.[5] Our lab has previously shown that the aberrant expression of MUC13 is associated with an enhanced tumorigenesis both *in vitro* and *in vivo* in ovarian cancer[6], CRC[7], and PanCa.[8] In all three cancers, MUC13 was associated with an increased cancer cell motility as shown through enhanced proliferation, colony formation, invasion, and migration. In addition, MUC13 was found to be significantly overexpressed in cancerous tissues as compared to their normal counterparts, indicating a singular role in cancer development.[6,9,10] Results from PanCa and CRC studies seem to indicate that MUC13 expression is higher in both advanced-stage and metastatic tumor tissues.[9,10]

In order to better assess changes in a cell's behavior, various biochemical assays exist to elucidate the specific causes of these changes. There is great interest to understand

biophysical information at an ultrastructural level to help judge cellular phenotypes. To accomplish this, over the past few decades a new technology has emerged that allows for biophysical characterization of cells. This technology is based on relatively recent advances in the field of atomic force microscopy. An atomic force microscope (AFM) is a type of scanning probe microscope that works by taking a sharp metallic probe attached to a flexible cantilever and bringing it into contact with or a short distance above the sample's surface and can generate very high-resolution three-dimensional topographies. Due to the direct interaction between the probe and the sample's surface, it is possible to use an AFM to perform additional analyses – one of the most widely used and promising (particularly for biological research) is quantifying physical parameters via nanoindentation.[11–13] With this technique, the probe is brought into contact with the sample and a set deformation is applied. A force curve is generated, and using this, several nanomechanical parameters can be quantified (namely, Young's modulus[14,15] and adhesion[16–18]). Young's modulus, also known as the elastic modulus, is a parameter that defines a material's stiffness, and is defined as stress (a force applied over a given area) divided by strain (the change in a material's length as compared to its original dimensions). Given this parameter, it is possible to determine key physical changes – the more force required to deform a material indicates a higher modulus, and by contrast, a lower force to deform indicates a reduced modulus.[19]

The application of nanoindentation to cancer cells leads to a new and exciting technique to help identify and potentially even diagnose cancer from a purely physical analysis.[20] The current consensus in scientific literature supports the notion that cancer cells are less rigid (i.e., they have a lower modulus) than their healthy cellular counterparts. In addition, cells with a higher metastatic potential have also generally been seen to have a lower rigidity as well. [14,21] However, there is limited research on the biophysical role of mucins and virtually none of this applied to PanCa. Therefore, we present our findings on the biophysical effects of MUC13 *via* genetically modified PanCa cells with over-expressed or knocked down MUC13 levels to determine if any significant biophysical changes can be identified. This will then be compared to the phenotypic effect of MUC13 on cancer cells to see if the expected correlation in literature is met.

2. Materials and Methods

2.1. Cell culture

Cell lines (HPNE, HPAF-II, BxPC-3, MIA PaCa-2, AsPC-1, Panc-1) were purchased from the American Type Culture Collection (ATCC, Manassas, VA, USA) and were maintained at 37°C/5% CO_2 in growth medium with 10% FBS (DMEM, Cat. No. 11965092; RPMI-1640, Cat. No. 11875–093; DMEM/Ham's F12, Cat. No. 11320033, Gibco). HPNE, MIA PaCa-2, and Panc-1 cells were grown in DMEM media; BxPC-3 and AsPC-1 cells were grown in RPMI; HPAF-II cells were grown in DMEM/F-12 media. Cells were grown in T-75 flasks until at least 70% confluent. Next, media was aspirated under a flow hood and trypsinized at 37ºC until cells were detached. The cells were then centrifuged at 1000 rpm for 5 min, counted, and seeded as needed for the various experiments discussed below.

2.2. Transfection of PanCa cells for altered MUC13 expression

Transfected models of MUC13 modulated cells for PanCa cells were generated using previously described protocols.[8] In brief, overexpressing models were generated using Panc-1 cells transfected with Lipofectamine 2000 per manufacturer's directions (Invitrogen). Knockdown cell lines were created with HPAF-II transfected with MUC13 specific shRNA lentiviral particles per manufacturer's instructions (Sigma).

2.3. PCR

Cells were collected and RNA was isolated using TRIzol reagent. Reverse transcription was then conducted using High-Capacity cDNA reverse transcriptase kit (ThermoFisher) according to manufacturer's protocol. After collecting cDNA, it was amplified using MUC13 and GAPDH-specific primers. Quantitative real-time PCR was done using SYBR Green Master Mix on a Roche LightCycler.

2.4. AFM Imaging and Nanoindentation

Cells were seeded in 60 mm dishes (Sarstedt, Model No. 83.3901, Numbrecht, Germany) and grown to 75% confluency. The cells were then gently washed with Phosphate Buffered Saline (PBS, 1X, pH 7.4) three times and fresh media was added. Cells were taken to the AFM (BioScope Resolve, Bruker; Billerica,MA,USA) and placed on a heated stage (37 ^{o}C) and allowed to equilibrate for 10–15 minutes. During this time, the probe (PFQNM-LC, Bruker) was calibrated *via* thermal tune. These probes are custom-made for live cell applications and have pre-calibrated spring constants, allowing for a simple, one-step calibration. Once calibrated, the probe was brought into contact with a cell and a ramp test was run to confirm proper contact. A force volume scan was then conducted over a small group of cells (128*128 resolution, 15Hz scan rate, 400 pN force setpoint, 4 μm ramp size) and repeated on several groups. All data was collected within a two-hour window for each plate. Force data was then analyzed in two separate ways: firstly, over the whole cell using at least 75% of the surface of each cell, and then a regional analysis was conducted, taking equally sized 25 μm^2 regions randomly selected at the nuclear, cytoplasmic, and peripheral regions. This difference is visually summarized in Figure 1. The data was averaged for each group from multiple cells in each group using NanoScope Analysis software (Bruker). These experiments were repeated in triplicate.

2.5. Aggregation assays

To determine the effect of MUC13 on cell-to-cell adhesion, aggregation assays were conducted. The original protocol can be found in one of our lab's previous publications.[6] The protocol was slightly modified for use in these experiments: briefly, 20,000 cells were suspended in a small bead of media (~25 μL) which was deposited onto the lid of a petri dish. The base of the petri dish was filled with PBS to prevent evaporation. The lid was then placed on the dish and incubated overnight at 37 ^{o}C. The next day the lid was inverted, and the bead was gently pipetted to disperse any larger aggregates. Photos were then promptly taken using optical microscopes (20x images taken on EVOS® FLoid Cell Imaging System, Cat. No. 447136; ThermoFisher, Waltham, MA, USA).

2.6. Statistical analysis

Analyses were conducted using unpaired, two-tailed Student's T-tests to assess the differences between relevant groups in the various experiments. All error bars used in the attached figures indicate the standard error of mean (SEM). The number of stars used on each graph relates to the level of significance - i.e., one star (*) indicates P-values below 0.05, two stars (**) values below 0.01, three stars (***) for values below 0.001, and items with four stars (****) indicate all P-values below 0.0001.

3. Results

3.1. Characterization of pancreatic cell lines

In this study, MUC13 modulation was conducted on PanCa cell line models to investigate its biophysical effects on these disease states. In order to assess the effects of MUC13, we first investigated the baseline characteristics on a panel of normal and cancerous pancreatic cells. Figure 2 outlines the results of analyzing this panel of cells. All cancerous cells were considerably softer than the reference normal cell line (HPNE). In addition, there is a noticeable trend in the cell lines with reduced differentiation status – as shown in Figure 2A, there is a further reduction in MIA PaCa-2, AsPC-1 and Panc-1 as compared to HPAF-II and BxPC-3, which are poorly differentiated and more well differentiated respectively.[22] Some minor differences were also seen in the membrane adhesiveness between these cells (Figure 2B), but in comparison to the large changes in membrane rigidity these were relatively minor.

Representative force maps for these cells (shown in Figure 2C) clearly show the difference in cellular rigidity and adhesion between these cell lines. MUC13 modulated cells were generated using the protocols outlined in the Methods section. Using PCR analysis, altered MUC13 expression was confirmed in these cell lines. Of the cell lines shown in Figure 2, HPAF-II was chosen for the knockout model as our lab has previously shown it has extensive MUC13 expression, while Panc-1 has shown minimal to no MUC13 expression, making it an ideal candidate for an overexpression model.[8]

3.2. Altered MUC13 expression exhibits significant biophysical effects on PanCa cells

Overexpression of MUC13 in Panc-1 cells (Figure 3A) gave results that theoretically agreed with the expected trends in literature, specifically that genetic changes that cause enhanced invasive or migratory potential reduce the cellular moduls.[23,24] Panc-1 MUC13 OE cells were significantly softer than their vector counterparts (Figure 3Bi). Overall, there was no significant change in membrane adhesion (Figure 3Ci).

A set of HPAF-II cells with MUC13 knockdown (Figure 4A) showed the opposite effect, i.e., an overall significant increase in was noted in the modulus (Figure 4Bi) as well as a highly significant increase in membrane adhesiveness (Figure 4Ci).

3.3. Differences in overall and regional nanomechanical analysis for MUC13-modulated cells

As discussed in the Methods section and shown in Figure 1, the MUC13 modulated cells were analyzed in an overall method (as seen in Figures 3 and 4) as well as a regional method, where data was collected in equally sized regions at the nuclear, cytoplasmic and peripheral regions. When looking at the regional data for Panc-1 MUC13 overexpressing cells, a significant reduction in the modulus was noted in the nuclear and cytoplasmic regions, and a significant reduction was noted in adhesion but only at the nuclear region (Figure 5A). For HPAF-II MUC13 knockout cells, the modulus was found to be significantly increased at the cytoplasmic and peripheral regions, and the cell has significantly higher membrane adhesion at all regions of the cell (Figure 5B). The data in Figures 3,4, and 5 shows that the trend between the overall and regional analyses are similar.

3.4. Increased MUC13 associated with reduced cellular aggregation

Aggregation assays were conducted on these cell lines to determine the effect of MUC13 on cell-to-cell cohesion. The results of these tests indicate that MUC13 plays a potent role in affecting this intercellular adhesion. It was shown that Panc-1 cells with overexpressed MUC13 were only loosely grouped to one another, while the vector control consistently stayed in tight clusters (Figure 6A). HPAF-II vector cells did show some inherent adhesiveness; however, it was observed to be in loosely connected clumps with several detaching cells. With MUC13 knockdown, there appeared to be a greater interconnectivity between the cells, and a clear sheet-like layer of cells was observed (Figure 6B).

4. Discussion

Multiple previous studies have shown that cancer cells have a reduced modulus when compared to their normal and noncancerous counterparts.[14,25,26] In addition, factors that enhance oncogenic phenotypes have also led to reductions in cancer cell rigidity.[23,27,28] It is thought that these changes are in part due to changes in the cytoskeleton of the cell.[29,30] Due to this, several studies have been conducted investigating the biophysical differences in cancerous and normal tissue as a means of rapid identification and diagnosis of cancer.[26,31,32]

Although various studies have been published detailing the biophysical effects of various genetic alterations or treatment with various compounds in both PanCa[23,33,34] and other gastrointestinal cancers such as CRC[35], there has been no study to date investigating the biophysical effect of MUC13 expression in these cancers. Based on the nanoindentation and additional supporting data discussed in this section, we can conclude that differential MUC13 expression has significant biophysical effects on PanCa cells.

As shown in Figure 2A, cancerous pancreatic cells have considerably lower rigidity compared to the normal reference cell line (HPNE). This is in agreement with the conventional consensus in the literature that cancerous cells are softer than their normal counterparts.[14,25,32] Although changes in membrane adhesion were also noted (Figure 2B),

they were not as large as the changes in cell rigidity. These changes are best visualized in the representative force maps (Figure 2C).

When observing the effect of MUC13 on the biophysical properties in these cells, PanCa cells gave the initially anticipated result. MUC13 overexpression led to a significant reduction in the cell modulus (Panc-1, Figure 3B), which is expected for changes leading to an increased oncogenicity. HPAF-II cells also showed the anticipated effect with MUC13 knockdown in the form of significant increases in both modulus and adhesion (Figures 4B,C).

Of note, there is a considerable change in the base rigidity of Panc-1 and HPAF-II after transfection has occurred. Specifically, the average rigidity of Panc-1 raised from approximately 2kPa to nearly 8kPa after transfection with the vector plasmids. In addition, HPAF-II dropped from around 14kPa to approximately 10kPa. It is unclear as to the exact mechanism behind this biophysical change; however, we speculate that the effects of stable transfection and antibiotic selection have caused considerable change in the cell which led to significant physical changes as well. Of note, at least one study has shown that transient transfection with siRNA led to minimal changes in biophysical properties[23], however this may be due to a lack of antibiotic selection pressure on the cells.

As mentioned above, the trends in the overall and regional analyses are similar. Regional data examining the nuclear, cytoplasmic, and peripheral regions individually may provide a clearer insight into some of the effects of MUC13 modulation on cancer cell phenotypes, especially when looking at changes at the periphery of the cell. Changes at this region may be more closely related to changes in the motility and adhesive properties in a two-dimensional culture, but all regions of the cell should need to be considered for three-dimensional effects, as evident by alterations in aggregation.

MUC13 seems to directly impede the ability of cells to aggregate with one another *in vitro*. This may be in part to its ability to impede with the association of cadherins between cells, impacting cell to cell adhesion and facilitating the dissociation and invasion of cancer cells from the primary tumor. Similar results previously published from our lab indicated a similar effect on MUC13 modified ovarian cancer cells; specifically, a reduced aggregation was seen with MUC13 overexpression as compared to the vector.[6] In addition, our lab has previously published data indicating an interaction between MUC13 and HER2 in PanCa cells, leading to an upregulation of its downstream pro-oncogenic pathways. This in turn is implicated in affecting various facets of oncogenicity, including disruption of integrins at the cell membrane, which can lead to a reduced interaction with the extracellular matrix.[36]

Furthermore, previous studies have shown an interaction between MUC13 and HER2 in PanCa cells. This is of note as HER2 is thought to be activated by MUC13, and in turn reduce the function of E-cadherin which would lower cell-cell adhesion.[6,8,36] This may partially explain why cells with overexpressed MUC13 have been shown to have enhanced motility, as removing E-cadherin from the surface of the cell frees β-catenin, which could then act as a transcription factor to propagate the EMT cycle.[37]

As shown from previously published data from our lab, knockdown of MUC13 in HPAF-II cells is associated with a reduction in clonogenic, invasive, migratory, and proliferative phenotypes. This supports the notion of reduced aggressiveness with an increased cellular modulus noted in MUC13 KO cells compared to their vector. By contrast, the overexpression of MUC13 in Panc-1 has the opposite effect, leading to an increase in proliferation and clonogenic potential[8] - this helps to support the notion that MUC13 increases cancer cell aggressiveness and leads to a reduction in cellular rigidity. Recently, our lab showed that in PanCa cells, MUC13 was associated with an increased glucose uptake and metabolism via stabilizing the Glut-1 protein, allowing cancer cells to utilize more glucose for various functions.[38]

Clinically, MUC13 has been shown to be associated with a poorer prognosis in PanCa. This was shown in recent research by Khan et al, where tissue samples showed a positive correlation between later stage disease and increased MUC13 expression. In addition, MUC13 was more pronounced in cancerous tissue compared to normal adjacent, and especially concentrated in higher stage (Stage III-IV) or metastatic tissue as demonstrated in one of our lab's previous reports.[9]

This effect does not appear to be limited to gastrointestinal cancers - as shown in our lab's previous work on ovarian cancer, MUC13 expression led to significant changes in cellular motility.[6] We can therefore hypothesize that based on the results from this study, a significant biophysical effect would occur, but studies would need to be run to see how MUC13 affects ovarian cancer cells.

These results indicate the potential of AFM-based nanoindentation for use as a clinical tool for cancer assessment. Using only the physical changes observed in tumor samples, it may one day be possible for pathologists to determine the course of a disease state by measuring physical changes over time and using these changes as prognostic indicators of disease progression.

5. Conclusion

Overall, MUC13 seems to impart significant biophysical changes associated with a promotion of increased metastatic potential. In this paper, we assessed the biophysical effects of MUC13 modulation on PanCa cells. These cells were first scanned in their native configuration to determine their baseline physical characteristics. With MUC13 modulation, significant changes were seen in the biophysical parameters for PanCa cells (modulus and adhesion) which correlated with previous phenotypic data produced from our lab. When taken together, these data help to show that MUC13 leads to an increased metastatic potential, which in turn softens the cell leading to an increase in its overall motility and reduction in cell-cell adhesion.

Acknowledgement

This work was partially supported by NIH R01CA210192, R01CA206069, R01CA204552, Herb Kosten Foundation, Memphis, College of Pharmacy/University of Tennessee Health Science, Center Seed/Instrument grant, and UTRGV-SOM start-up funds.

References

1. Siegel RL, Miller KD, Jemal A. Cancer statistics, 2018 CA Cancer J Clin. 2018;68(1):7–30. doi: 10.3322/caac.21442. [PubMed: 29313949]
2. Cavanna L, Stroppa EM, Citterio C, et al. Modified FOLFIRINOX for unresectable locally advanced/metastatic pancreatic cancer. A real-world comparison of an attenuated with a full dose in a single center experience. Onco Targets Ther. 2019;12:3077–3085. doi:10.2147/OTT.S200754. [PubMed: 31118666]
3. Kufe DW. Mucins in cancer: function, prognosis and therapy. Nat Rev Cancer. 2009;9(12):874–885. doi:10.1038/nrc2761. [PubMed: 19935676]
4. van Putten JPM, Strijbis K. Transmembrane Mucins: Signaling Receptors at the Intersection of Inflammation and Cancer. J Innate Immun. 2017;9(3):281–299. doi:10.1159/000453594. [PubMed: 28052300]
5. Maher DM, Gupta BK, Nagata S, Jaggi M, Chauhan SC. Mucin 13: structure, function, and potential roles in cancer pathogenesis. Mol Cancer Res. 2011;9(5):531–537. doi: 10.1158/1541-7786.MCR-10-0443. [PubMed: 21450906]
6. Chauhan SC, Vannatta K, Ebeling MC, et al. Expression and functions of transmembrane mucin MUC13 in ovarian cancer. Cancer Res. 2009;69(3):765–774. doi:10.1158/00085472.CAN-08-0587. [PubMed: 19176398]
7. Gupta BK, Maher DM, Ebeling MC, et al. Functions and regulation of MUC13 mucin in colon cancer cells. J Gastroenterol. 2014;49(10):1378–1391. doi:10.1007/s00535-013-0885-z. [PubMed: 24097071]
8. Chauhan SC, Ebeling MC, Maher DM, et al. MUC13 mucin augments pancreatic tumorigenesis. Mol Cancer Ther. 2012;11(1):24–33. doi:10.1158/1535-7163.MCT-110598. [PubMed: 22027689]
9. Khan S, Zafar N, Khan SS, et al. Clinical significance of MUC13 in pancreatic ductal adenocarcinoma. Hpb. 2018;20(6):563–572. doi:10.1016/j.hpb.2017.12.003. [PubMed: 29352660]
10. Gupta BK, Maher DM, Ebeling MC, et al. Increased expression and aberrant localization of mucin 13 in metastatic colon cancer. J Histochem Cytochem. 2012;60(11):822–831. doi: 10.1369/0022155412460678. [PubMed: 22914648]
11. Binnig G, Quate CF. Atomic Force Microscope. Phys Rev Lett. 1986;56(9):930–933. doi:10.1103/PhysRevLett.56.930. [PubMed: 10033323]
12. Li M, Liu L, Xi N, Wang Y. Atomic force microscopy studies on cellular elastic and viscoelastic properties. Sci China Life Sci. 2018;61(1):57–67. doi:10.1007/s11427-0169041-9. [PubMed: 28667516]
13. Yallapu MM, Katti KS, Katti DR, et al. The roles of cellular nanomechanics in cancer. Med Res Rev. 2015;35(1):198–223. doi:10.1002/med.21329. [PubMed: 25137233]
14. Lekka M Discrimination Between Normal and Cancerous Cells Using AFM. Bionanoscience. 2016;6(1):65–80. doi:10.1007/s12668-016-0191-3. [PubMed: 27014560]
15. Luo Q, Kuang D, Zhang B, Song G. Cell stiffness determined by atomic force microscopy and its correlation with cell motility. Biochim Biophys Acta - Gen Subj. 2016;1860(9):1953–1960. doi: 10.1016/j.bbagen.2016.06.010.
16. Park S, Lee YJ. AFM-based dual nano-mechanical phenotypes for cancer metastasis. J Biol Phys. 2014;40(4):413–419. doi:10.1007/s10867-014-9353-0. [PubMed: 24980951]
17. Abduljauwad SN, Ahmed H ur R. Enhancing cancer cell adhesion with clay nanoparticles for countering metastasis. Sci Rep. 2019;9(1):1–12. doi:10.1038/s41598-019-42498-y. [PubMed: 30626917]
18. Kim H, Yamagishi A, Imaizumi M, et al. Quantitative measurements of intercellular adhesion between a macrophage and cancer cells using a cup-attached AFM chip. Colloids Surfaces B Biointerfaces. 2017;155:366–372. doi:10.1016/j.colsurfb.2017.04.039. [PubMed: 28454065]
19. Gavara N A beginner's guide to atomic force microscopy probing for cell mechanics. Microsc Res Tech. 2017;80(1):75–84. doi:10.1002/jemt.22776. [PubMed: 27676584]
20. Swaminathan V, Mythreye K, O'Brien ET, Berchuck A, Blobe GC, Superfine R. Mechanical stiffness grades metastatic potential in patient tumor cells and in cancer cell lines. Cancer Res. 2011;71(15):5075–5080. doi:10.1158/0008-5472.CAN-11-0247. [PubMed: 21642375]

21. Cross SE, Jin YS, Rao J, Gimzewski JK. Nanomechanical analysis of cells from cancer patients. Nat Nanotechnol. 2007;2(12):780–783. doi:10.1038/nnano.2007.388. [PubMed: 18654431]
22. Deer EL, González-Hernández J, Coursen JD, et al. Phenotype and genotype of pancreatic cancer cell lines. Pancreas. 2010;39(4):425–435. doi:10.1097/MPA.0b013e3181c15963. [PubMed: 20418756]
23. Lee Y, Koay EJ, Zhang W, et al. Human equilibrative nucleoside transporter-1 knockdown tunes cellular mechanics through epithelial-mesenchymal transition in pancreatic cancer cells. PLoS One. 2014;9(10). doi:10.1371/journal.pone.0107973.
24. Lin HH, Lin HK, Lin IH, et al. Mechanical phenotype of cancer cells: Cell softening and loss of stiffness sensing. Oncotarget. 2015;6(25):20946–20958. doi:10.18632/oncotarget.4173.
25. Stylianou A, Kontomaris SV, Grant C, Alexandratou E. Atomic force microscopy on biological materials related to pathological conditions. Scanning. 2019;2019. doi:10.1155/2019/8452851.
26. Lekka M, Gil D, Pogoda K, et al. Cancer cell detection in tissue sections using AFM. Arch Biochem Biophys. 2012;518(2):151–156. doi:10.1016/j.abb.2011.12.013. [PubMed: 22209753]
27. Ku M, Kim HJ, Yau SY, et al. Microsphere-Based Nanoindentation for the Monitoring of Cellular Cortical Stiffness Regulated by MT1-MMP. Small. 2018;14(41):1–10. doi:10.1002/smll.201803000.
28. Sun J, Luo Q, Liu L, Song G. Low-level shear stress induces differentiation of liver cancer stem cells via the Wnt/β-catenin signalling pathway. Exp Cell Res. 2019;375(1):90–96. doi:10.1016/j.yexcr.2018.12.023. [PubMed: 30599139]
29. Yamagishi A, Susaki M, Takano Y, et al. The Structural Function of Nestin in Cell Body Softening is Correlated with Cancer Cell Metastasis. Int J Biol Sci. 2019;15(7):1546–1556. doi:10.7150/ijbs.33423. [PubMed: 31337983]
30. Pei W, Chen J, Wang C, et al. Regional biomechanical imaging of liver cancer cells. J Cancer. 2019;10(19):4481–4487. doi:10.7150/jca.32985. [PubMed: 31528212]
31. Peñuela LA, Fulcheri E, Vellone VG, et al. Atomic force microscopy: a promising aid in diagnosis of uterine smooth muscle neoplasms. Am J Obstet Gynecol. 2019;(October):362–364. doi:10.1016/j.ajog.2019.05.013. [PubMed: 31121140]
32. Stylianou A, Lekka M, Stylianopoulos T. AFM assessing of nanomechanical fingerprints for cancer early diagnosis and classification: from single cell to tissue level. Nanoscale. 2018. doi:10.1039/C8NR06146G.
33. Mezencev R, Wang L, Xu W, et al. Molecular analysis of the inhibitory effect of Nacetyl-L-cysteine on the proliferation and invasiveness of pancreatic cancer cells. Anticancer Drugs. 2013;24(5):504–518. doi:10.1097/CAD.0b013e32836009d7. [PubMed: 23511429]
34. Kulkarni T, Tam A, Mukhopadhyay D, Bhattacharya S. AFM study: Cell cycle and probe geometry influences nanomechanical characterization of Panc1 cells. Biochim Biophys Acta - Gen Subj. 2019;1863(5):802–812. doi:10.1016/j.bbagen.2019.02.006. [PubMed: 30763604]
35. Liu H, Wang N, Zhang Z, Wang H, Du J, Tang J. Effects of Tumor Necrosis Factor-α on Morphology and Mechanical Properties of HCT116 Human Colon Cancer Cells Investigated by Atomic Force Microscopy. Scanning. 2017;2017:2027079. doi:10.1155/2017/2027079.
36. Khan S, Sikander M, Ebeling MC, et al. MUC13 interaction with receptor tyrosine kinase HER2 drives pancreatic ductal adenocarcinoma progression. Oncogene. 2016;(May):1–10. doi:10.1038/onc.2016.218.
37. Conant JL, Peng Z, Evans MF, Naud S, Cooper K. Sarcomatoid renal cell carcinoma is an example of epithelial-mesenchymal transition. J Clin Pathol. 2011;64(12):1088–1092. doi:10.1136/jclinpath-2011-200216. [PubMed: 22003062]
38. Kumari S, Khan S, Gupta SC, et al. MUC13 contributes to rewiring of glucose metabolism in pancreatic cancer. Oncogenesis. 2018;7(2). doi:10.1038/s41389-018-0031-0.

Highlights

- Pancreatic cancer is known to aberrantly express mucin protein MUC13
- High levels of MUC13 are associated with enhanced aggressiveness in multiple cancers
- Nanomechanical analysis of MUC13 modulated cells shows unique biophysical changes
- Observed physical changes agree with literature consensus on reduced modulus in more aggressive or invasive cells

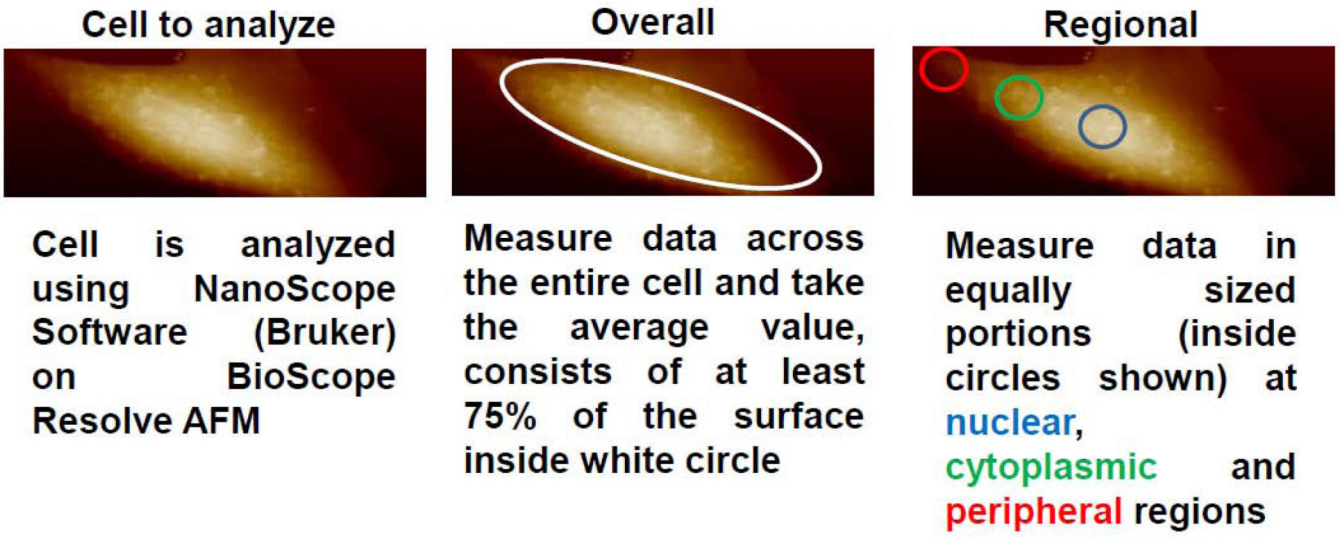

Figure 1: Schematic overview of different analysis methods used in this study.

Cells were scanned and analyzed for overall data (taking an average value of at least 75% of the surface of the cell) or in a compartmentalized manner (measuring data in equally sized, randomly selected portions of the nuclear, cytoplasmic, and peripheral regions).

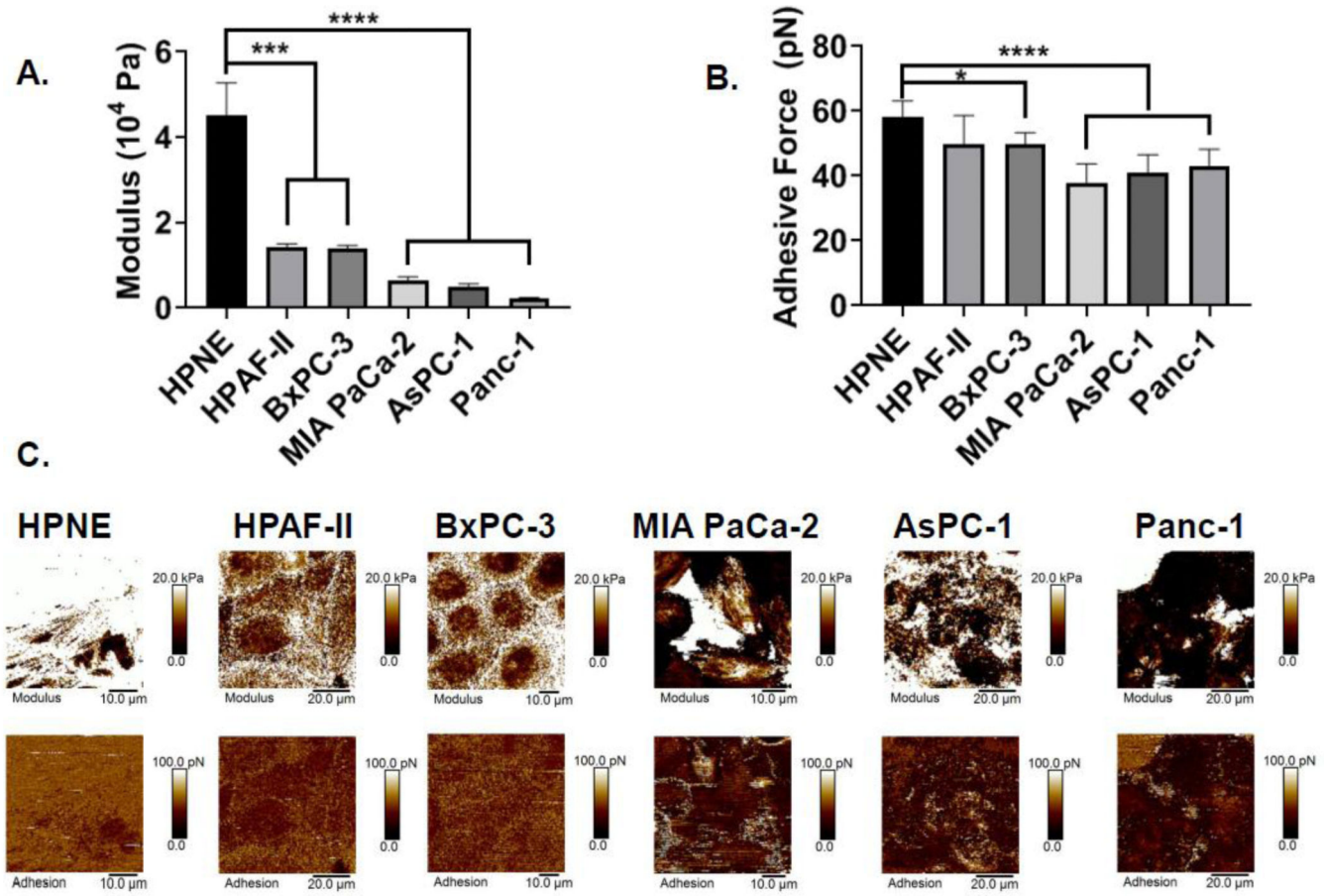

Figure 2: Characterization of normal and cancerous pancreatic cells.

(A) Modulus data for a panel of normal and cancerous pancreatic cells. (B) Adhesion data for the pancreatic cell panel. (C) Representative force images showing relative changes in physical parameters between cell lines.

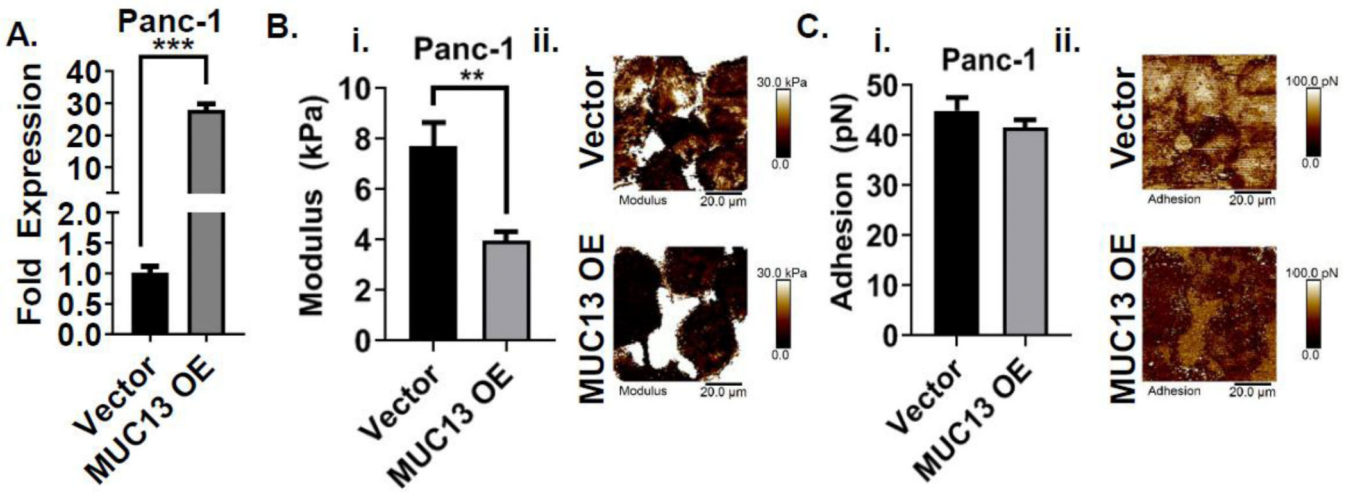

Figure 3: Effect of MUC13 overexpression on PanCa biophysical properties.

(A) PCR data showing increased mRNA with MUC13 overexpressed cells. (B) Effect of MUC13 overexpression on modified Panc-1 cell rigidity (i). Representative force maps show changes in modulus across the surface of the cell (ii). (C) Effect of MUC13 overexpression on modified Panc-1 adhesiveness (i). Representative force maps show changes in adhesion across the surface of the cell (ii).

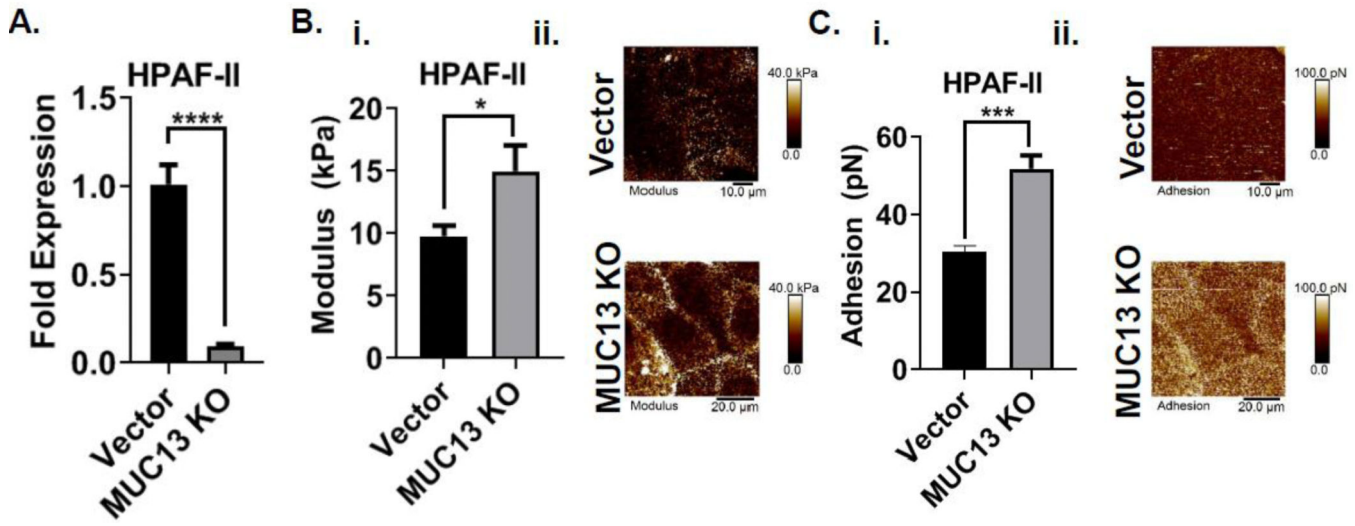

Figure 4: Effect of MUC13 knockdown on PanCa biophysical properties.

(A) PCR results showing reduced mRNA levels with MUC13 knockdown. (B) Effect of MUC13 knockdown on rigidity of modified HPAF-II cells (i). Representative force maps showing changes in rigidity across the surface of the cell (ii). (C) Effect of MUC13 knockdown on adhesion of modified HPAF-II cells (i). Representative force maps showing the changes in adhesion across the surface of the cell (ii).

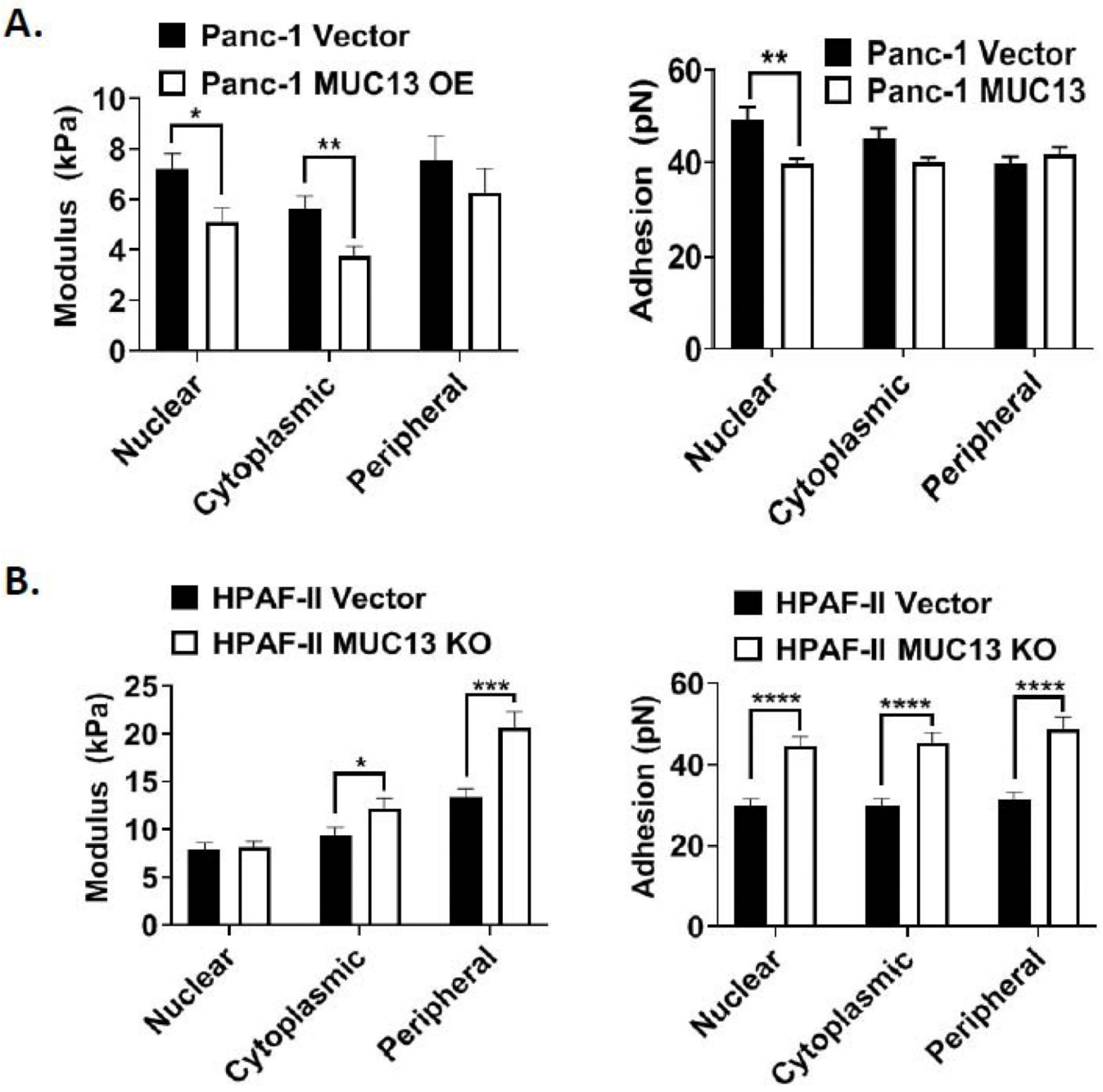

Figure 5: Regional nanomechanical analysis of MUC13-modulated PanCa cells.

(A) Regional nanoindentation data for Panc-1 MUC13 overexpressed cells showing localized changes at the nuclear, cytoplasmic, and peripheral regions of the cell surface. (B) Regional nanoindentation data for HPAF-II MUC13 knockdown cells showing localized changes at the nuclear, cytoplasmic, and peripheral regions of the cell surface.

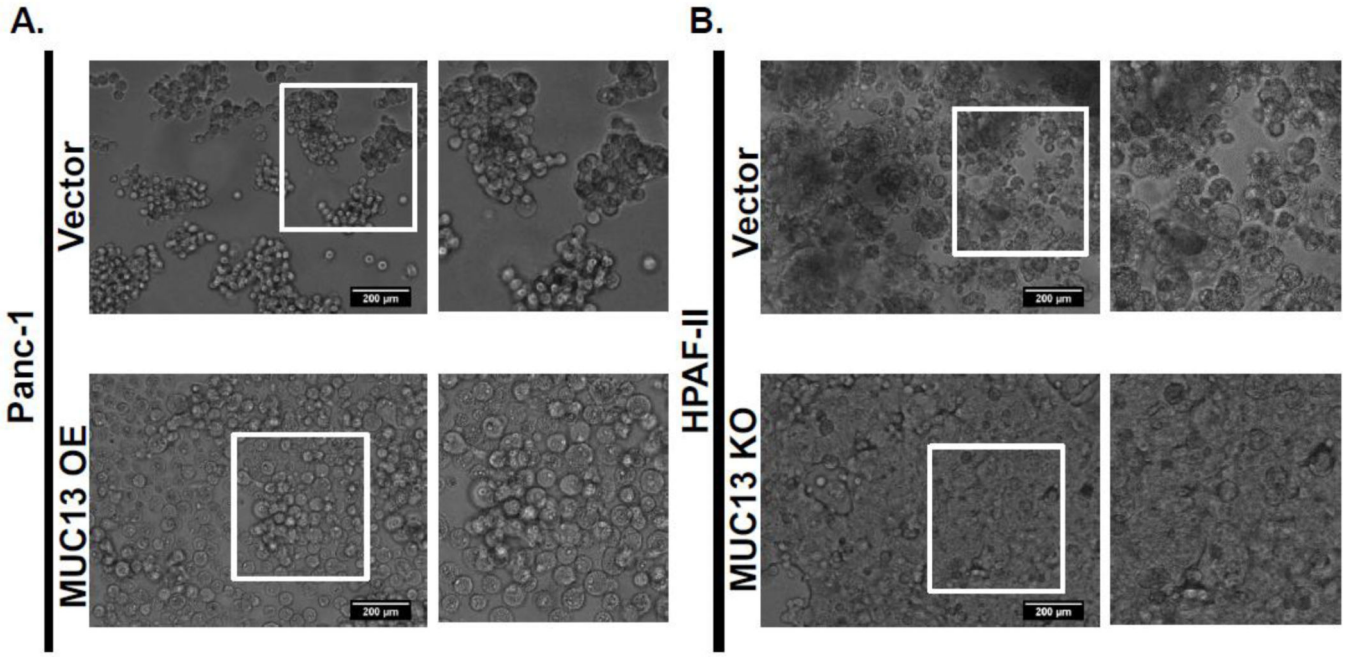

Figure 6: Effect of MUC13 modulation on cellular aggregation.

(A) Panc-1 cells show decreased cell-cell adhesion with MUC13 overexpression. (B) HPAF-II cells show increased cell-cell adhesion with MUC13 knockdown. Cells were imaged at 20x magnification. Representative groups of cells are highlighted with white squares and magnified images are detailed on the right of each image to show detailed effect of MUC13 on cellular aggregation.